The Structure and Organization of Synthetic Putative Membranous Segments of ROMK1 Channel in Phospholipid Membranes

Iris Ben-Efraim and Yechiel Shai
Department of Membrane Research and Biophysics, Weizmann Institute of Science, Rehovot, 76100 Israel

ABSTRACT The hydropathy plot of ROMK1, an inwardly rectifying K^+ channel, suggests that the channel contains two transmembrane domains (M1 and M2) and a linker between them with significant homology to the H5 pore region of voltage-gated K^+ channels. To gain structural information on the pore region of the ROMK1 channel, we used a spectrofluorimetric approach and characterized the structure, the organization state, and the ability of the putative membranous domains of the ROMK1 channel to self-assemble and coassemble within lipid membranes. Circular dichroism (CD) spectroscopy revealed that M1 and M2 adopt high α-helical structures in egg phosphatidylcholine small unilamellar vesicles and 40% trifluoroethanol (TFE)/water, whereas H5 is not α-helical in either egg phosphatidylcholine small unilamellar vesicles or 40% TFE/water. Binding experiments with 4-fluoro-7-nitrobenz-2-oxa-1,3-diazole (NBD)-labeled peptide demonstrated that all of the peptides bind to zwitterionic phospholipid membranes with partition coefficients on the order of 10^5 M^{-1}. Tryptophan quenching experiments using brominated phospholipids revealed that M1 is dipped into the hydrophobic core of the membrane. Resonance energy transfer (RET) measurements between fluorescently labeled pairs of donor (NBD)/acceptor (rhodamine) peptides revealed that H5 and M2 can self-associate in their membrane-bound state, but M1 cannot. Moreover, the membrane-associated nonhelical H5 serving as a donor can coassemble with the α-helical M2 but not with M1, and M1 can coassemble with M2. No coassembly was observed between any of the segments and a membrane-embedded α-helical control peptide, pardaxin. The results are discussed in terms of their relevance to the proposed topology of the ROMK1 channel, and to general aspects of molecular recognition between membrane-bound polypeptides.

INTRODUCTION

Potassium ion channels, found in various eukaryotic cells, are functionally diverse and thus play an important role in a broad spectrum of processes in excitable and nonexcitable cells (Hille, 1992). These proteins form K^+-selective channels that can be rapidly opened or closed by changes in transmembrane potentials. During the past few years several potassium channels belonging to the voltage-gated family have been cloned. They include K^+ channels expressed by the *Shaker*, *Shab*, and *Shaw* loci of *Drosophila* (Schwarz et al., 1988; Butler et al., 1989), as well as their homologs from rodent brain (Schwarz et al., 1986; Stühmer et al., 1989). These *Shaker*-type K^+ channels are characterized by the presence of six putative membrane-spanning segments (S1-S6), a putative voltage sensor (S4), and an S5-S6 linker (H5) region. The functional channel has been shown to be formed through tetrameric associations (MacKinnon, 1991) in vitro as well as in vivo (Sheng et al., 1993; Wang et al., 1993). Recently the cDNA cloning in *Xenopus* oocytes of five inwardly rectifying potassium channels, namely ROMK1 (Ho et al., 1993), IRK1 (Kubo et al., 1993a), GIRK1/KGB (Dascal et al., 1993; Kubo et al., 1993b), K_{ATP} (Ashford et al., 1994), and RACTK1 (Suzuki et al., 1994), has revealed the primary structure of these channels.

Inwardly rectifying K^+ channels are not gated by membrane potential, but conduct an inward K^+ current at hyperpolarizing membrane potentials. Because of their rectification properties, these channels play an important role in regulating the resting membrane potential and electrical excitability of cells in a variety of tissues, including brain and heart (Hille, 1992). Interestingly, hydropathic analysis of these inwardly rectifying channels predicts only two potential transmembrane domains, namely M1 and M2. Furthermore, significant similarity to the H5 pore region of voltage-gated K^+ channels (Miller, 1991) was found for a segment between M1 and M2 (44% similarity for ROMK1; Ho et al., 1993). Because of this similarity the H5 regions of ROMK1, IRK1, GIRK1/KGB, and K_{ATP} are believed to form the ion pore and to give rise to K^+ selectivity and cation blocking pharmacology (Kaback, 1992; Kubo et al., 1993a,b; Ashford et al., 1994). Because some amino acid residues of M1 and M2 are also identical to the corresponding residues in S5 and S6, which are highly conserved among voltage-gated K^+ channels, Kubo and colleagues proposed that IRK1 channels are structurally analogous to an inner core of the *Shaker* superfamily channels (Kubo et al., 1993a). In this structure the lining of the channel pore is formed by the H5, M1, and M2 regions, but the S1-S4 transmembrane domains that form an outer shell of the *Shaker*-type channel structure are lacking. The possible connection between these two classes of K^+ channels has been investigated by deletion of the transmembrane domains S1 to S4 of a delayed rectifier RCK1 (K v1.1) K^+

Received for publication 30 January 1996 and in final form 11 October 1996.

Address reprint requests to Dr. Yechiel Shai, Department of Membrane Research and Biophysics, Weizmann Institute of Science, Rehovot, 76100 Israel. Tel.: 972-8-9342711; Fax: 972-8-9344112; E-mail: bmshai@weizmann.weizmann.ac.il.

0006-3495/97/01/85/12 $2.00

channel and relegation of the amino terminal domain to the transmembrane region S5 (Tytgat et al., 1994). Functional expression of the mutant channel revealed that the mutant channel is activated upon hyperpolarization, showing a strong inward rectification. This phenotypical change associated with the removal of the transmembrane domains S1-S4 suggests a structural link between inward rectifier and *Shaker* superfamily ion channels (Tytgat et al., 1994).

Here, synthetic peptides were utilized to gain information on the secondary structure and the organization within the membrane of the putative transmembrane domains of the ROMK1 K^+ channel. Three peptides corresponding to M1, M2, and H5 were synthesized, fluorescently labeled, and structurally and functionally characterized. The secondary structure of the segments was characterized using circular dichroism (CD), and their ability to bind to phospholipid vesicles was monitored with 7-nitrobenz-2-oxa-1,3-diazole-4-yl (NBD)-labeled peptides. Tryptophan quenching experiments using brominated phospholipids were done with the tryptophan-containing M1. Fluorescence resonance energy transfer (RET) experiments were then performed with donor/acceptor-labeled segments to assess their ability to self-assemble and to coassemble within the membrane. The data reveal that: 1) all of the segments bind strongly to the membrane; 2) M1 and M2 adopt highly α-helical structures, whereas H5 is not α-helical; 3) H5 and M2 can self-associate in their membrane-bound state but M1 cannot; 4) membrane-associated H5 can coassemble with M2 but not with M1; and 5) M1 can coassemble with M2. No coassembly was observed between any of the segments and a membrane-embedded α-helical control peptide, pardaxin. The results are discussed in terms of their relevance to the proposed topology of the ROMK1 channel, and to general aspects of molecular recognition between membrane-bound polypeptides.

EXPERIMENTAL PROCEDURES

Materials

Butyloxycarbonyl-(amino acid)-(phenylacetamido)methyl resins were purchased from Applied Biosystems (Foster City, CA), and butyloxycarbonyl (BOC) amino acids were obtained from Peninsula Laboratories (Belmont, CA). Other reagents for peptide synthesis were obtained from Sigma. Egg phosphatidylcholine (PC) was purchased from Lipid Products (South Nutfield, England). Cholesterol (extra pure) purchased from Merck (Darmstadt, Germany) was recrystallized twice from ethanol. Brominated phospholipids (BrPC) were purchased from Avanti Polar Lipids. 5- (and 6)-Carboxytetramethylrhodamine succinimidyl ester (Rho-Su) was obtained from Molecular Probes (Eugene, OR). NBD-F (4-fluoro-7-nitrobenz-2-oxa-1,3-diazole) was obtained from Sigma. All other reagents were of analytical grade. Buffers were prepared using double glass-distilled water.

Peptide synthesis, fluorescent labeling, and purification

Peptides were synthesized by a solid-phase method on (phenylacetamido)methyl-amino acid resin (0.15 meq) (Merrifield et al., 1982), as previously described (Shai et al., 1991). Double coupling was carried out with freshly prepared 1-hydroxybenzotriazole active esters of BOC amino acids. The synthetic polypeptides were purified to a chromatographic homogeneity of >98% by reverse-phase high-performance liquid chromatography on an analytical C_4 Vydac column 4.6 mm × 250 mm (pore size of 300 Å). The column was eluted in 40 min using linear gradients of acetonitrile in water in the presence of 0.1% trifluoroacetic acid (v/v). The flow rate was 0.6 ml/min, and the gradients were 30–90% for M1 and 25–80% for M2 and H5. The peptides were subjected to amino acid analysis to confirm their composition.

Labeling of the polypeptides' N-terminus was achieved by labeling resin-bound polypeptide in its fully protected form as follows. Resin-bound peptide (30–40 mg, i.e., 10–25 μmol) was treated with trifluoroacetic acid (50% v/v in methylene chloride) to remove the BOC protecting group from the N-terminal amino group of the attached peptide (Rapaport and Shai, 1991). The resin-bound peptides were then reacted with either 1) 5–7 equivalents of 5- (and 6)-carboxytetramethylrhodamine succinimidyl ester (Rho-Su) in dimethyl formamide (DMF) containing 3% v/v triethylamine, or 2) 5–7 equivalents of 4-fluoro-7-nitrobenz-2-oxa-1,3-diazole (NBD-F) in DMF. These reactions led to the formation of resin-bound N1-Rho or N^1-NBD-peptides, respectively. After 24 h, the resins were washed thoroughly with DMF and then with methylene chloride. After the dinitrophenyl and formyl protecting groups were removed from the histidine and tryptophan residues, the peptides were cleaved from the resin with hydrogen fluoride. The cleaved peptides were precipitated with ether and purified by reverse-phase high-performance liquid chromatography as described above.

Preparation of small unilamellar vesicles

Small unilamellar vesicles (SUVs) were used in the NBD shift and tryptophan quenching experiments, as well as in the binding experiments and CD measurements to decrease the light scattering effects. SUVs were prepared from PC by sonication. Briefly, dry lipid and cholesterol were dissolved in $CHCl_3$:MeOH (2:1 v/v) to yield mixtures that contained 10% w/w of cholesterol (cholesterol was included to reduce the curvature of the SUV vesicles; Lelkes, 1984). The solvents were evaporated under a stream of nitrogen, and the lipids (at a concentration of 7.2 mg/ml) were resuspended in buffer (50 mM Na_2SO_4, 25 mM HEPES-SO_4^{-2}, pH 6.8) by vortex mixing. The resulting lipid dispersion was sonicated (10–30 min) in a bath-type sonicator (G1125SP1 sonicator; Laboratory Supplies Company, Hicksville, NY) until the turbidity had cleared. The lipid concentration of the solution was determined by phosphorus analysis (Bartlett, 1959). Vesicles were visualized after negative staining with uranyl acetate, using a JEOL JEM 100B electron microscope (Japan Electron Optics Laboratory Co., Tokyo, Japan). Vesicles were shown to be unilamellar, with an average diameter of 20–40 nm (Papahadjopoulos and Miller, 1967; Rapaport and Shai, 1992).

Preparation of large unilamellar vesicles

LUVs were used in the resonance energy transfer experiments to increase the distance between donor and acceptor molecules on two opposite sites of a vesicle. LUV were prepared from phospholipids by extrusion (Hope et al., 1985). Dry lipids were hydrated in buffer and dispersed by vortexing to produce multilamellar vesicles. The lipid suspension was freeze-thawed 10 times and then extruded through polycarbonate membranes three times with 0.4-μm pore diameter membranes and then eight times with 0.1-μm pore diameter membranes (Poretics Corp., Livermore, CA). The size distribution of the vesicles was determined by dynamic light scattering in a Malvern 4700 submicron particle analyzer. The mean diameter was found to be 113 nm. The lipid concentrations of the liposome suspensions were determined by phosphorus analysis (Bartlett, 1959).

CD spectroscopy

The CD spectra of the peptides were measured in 40% trifluoroethanol (TFE) and with PC SUV using a Jasco J-500A spectropolarimeter that had

been calibrated with (+)-10-camphorsulfonic acid. Films containing lipids and peptides were prepared as follows: PC lipids were dissolved in chloroform and peptides were dissolved in methanol. Both solutions were subsequently mixed and the solvent was removed by a stream of nitrogen. The dry film was hydrated with 1 ml of buffer (50 mM Na_2SO_4, 25 mM HEPES-SO_4^{-2}, pH 6.8) and SUV were prepared by sonication. The spectra were scanned at 23°C in a capped quartz optical cell with a 0.5-mm path length. Spectra were obtained at wavelengths of 250 to 200–190 nm. Four scans were performed at a scan rate of 20 nm/min, a sampling interval of 0.2 nm, and a peptide concentration ranging from 1.0×10^{-5} M to 1.6×10^{-5} M in 40% TFE and 3.0×10^{-5} M in PC SUV (3 mM). The peptide to lipid molar ratio was 1:100.

Fractional helicities (Greenfield and Fasman, 1969; Wu et al., 1981) were calculated as follows:

$$f_h = ([\theta]_{222} - [\theta]^0_{222})/[\theta]^{100}_{222},$$

where $[\theta]_{222}$ is the experimentally observed mean residue ellipticity at 222 nm, and values for $[\theta]^0_{222}$ and $[\theta]^{100}_{222}$, corresponding to 0% and 100% helix content at 222 nm, were estimated to be 2000 and 30,000 deg·cm^2/dmol, respectively (Chen et al., 1974; Wu et al., 1981).

NBD fluorescence measurements

Peptides were incorporated into PC vesicles as follows. To a solution of PC SUV (155 nmol of phospholipids containing 10% w/w of cholesterol and dissolved in 20 μl of buffer [50 mM Na_2SO_4, 25 mM HEPES-SO_4^{-2}, pH 6.8]) was added 1 μl dimethyl sulfoxide (DMSO) solution containing 0.04 nmol of a particular NBD-labeled peptide, namely M1, M2, or H5, thus establishing a lipid/peptide ratio of 3875:1. Because the fluorescence of the NBD moiety reached its maximum intensity at this lipid/peptide molar ratio, it is assumed that all of the peptide was bound to the vesicles. After a 2-min incubation, an emission spectrum of the NBD group was recorded in three separate experiments using a Perkin-Elmer LS-50B spectrofluorometer, with the excitation set at 470 nm (5-nm slit).

Tryptophan quenching experiments

The environmentally sensitive tryptophan has been utilized previously in combination with brominated phospholipids for the evaluation of peptide localization in the membrane (Bolen and Holloway, 1990; De Kroon et al., 1990; Gonzalez-Manas et al., 1992). M1, which contains two tryptophan residues, was incorporated into PC vesicles as follows: 50% PC, 40% BrPC, and 10% cholesterol (W/W) (310 nmol phospholipids) were dissolved in $CHCl_3$:MeOH (2:1 v/v), and M1 peptide (0.5 nmol) was dissolved in methanol. The two solutions were mixed together, thus establishing a lipid/peptide ratio of 610:1, followed by the evaporation of the solvents by a stream of nitrogen. The dry film was hydrated with 200 μl of buffer (50 mM Na_2SO_4, 25 mM HEPES-SO_4^{-2}, pH 6.8), and SUV liposomes were prepared by sonication. An emission spectrum of the tryptophan was recorded using a Perkin-Elmer LS-50B spectrofluorometer, with the excitation set at 280 nm (5-nm slit), in three separate experiments. Measurements were performed in a 1-cm path-length quartz cuvette in a final reaction volume of 2 ml.

Binding experiments

The environmentally sensitive NBD fluorophore has been utilized previously for polarity and binding studies (Frey and Tamm, 1990; Rapaport and Shai, 1991; Pouny et al., 1992; Ben-Efraim et al., 1993). The binding experiments were conducted in two different ways. Briefly, either PC SUVs were added successively to 0.1 μM NBD-labeled peptide at 24°C, or alternatively, 0.04 nmol of NBD-labeled peptides (1 μl in DMSO) was added to increasing concentrations of PC SUV (50 μl in buffer) in separate Eppendorf tubes, followed by dilution of the solution to 400 μl. The later method should minimize aggregation of peptides in solutions. The two methods gave similar results. Fluorescence intensities were measured in five separate experiments as a function of the lipid/peptide molar ratio on a Perkin-Elmer LS-50B spectrofluorometer. Excitation was set at 470 nm using a 10-nm slit, and emission was set at 530 nm using a 5-nm slit. To determine the extent of the lipids' contribution to any given signal, the readings observed when unlabeled peptides were titrated with lipid vesicles were subtracted as background from the recorded fluorescence intensities. The binding isotherms were analyzed as partition equilibria (Schwarz et al., 1986, 1987; Rizzo et al., 1987; Beschiaschvili and Seelig, 1990; Rapaport and Shai, 1991), using the following formula:

$$X^*_b = K^*_p C_f,$$

where X^*_b is defined as the molar ratio of bound peptide per 60% of the total lipid, assuming that the peptides were initially partitioned only over the outer leaflet of the SUV as previously suggested (Beschiaschvili and Seelig, 1990), K^*_p corresponds to the partition coefficient, and C_f represents the equilibrium concentration of free peptide in the solution. To calculate X_b, F_∞ (the fluorescence signal obtained when all of the peptide is bound to lipid) was extrapolated from a double reciprocal plot of F (total peptide fluorescence) versus C_L (total concentration of lipids) (Schwarz et al., 1986). Knowing the fluorescence intensities of unbound peptide, F_0, as well as of bound peptide, F, the fraction of membrane bound peptide, f_b, can be calculated using the formula

$$f_b = (F - F_0)/(F_\infty - F_0).$$

Having calculated the value of f_b, it is then possible to calculate C_f, as well as the extent of peptide binding, X^*_b. The curves resulting from plotting X_b* versus free peptides, C_f, are referred to as the conventional binding isotherms.

Resonance energy transfer experiments

Peptides were incorporated into PC vesicles as follows. To solutions of PC LUV (10:1 lipid/cholesterol molar ratio and 63 nmol of phospholipids in 40 μl of buffer) in separate Eppendorf tubes were added 1–2-μl DMSO solutions containing 0.016 nmol of each of the NBD-labeled peptides, namely M1, M2, and H5 (donor), 1) alone or 2) followed by the addition of 0.016 nmol of rhodamine-labeled peptides (acceptor) or 3) followed by the addition of 0.048 nmol of unlabeled M1, M2, and H5. The experiments were repeated three to five times for each concentration, with the standard deviation being ~3%. Before the acceptor molecules were added, the vesicle solutions containing donor molecules were vortexed thoroughly. After the addition of acceptor molecules, the mixtures were diluted to 0.4 ml with 50 mM Na_2SO_4, 25 mM HEPES-SO_4^{-2}, pH 6.8. Fluorescence spectra were obtained at room temperature in either a SLM-8000 spectrofluorometer or a Perkin-Elmer LS-50B spectrofluorometer, with the excitation monochromator set at 460 nm and a 5-nm slit width. Measurements were performed in a 0.4-cm path length quartz cuvette in a final reaction volume of 0.4 ml. Although the excitation maximum for NBD is 470 nm, a lower wavelength was chosen to minimize the excitation of tetramethylrhodamine (Harris et al., 1991).

The efficiency of energy transfer (E) was determined by calculating the decrease in the quantum yield of the donor due to the addition of an acceptor. E was obtained experimentally from the ratio of the fluorescence intensities of the donor in the presence (I_{da}) and in the absence (I_d) of the acceptor at the emission wavelength of the donor, after correcting for membrane light scattering and the contribution of the acceptor's emission. The percentage value of E is given by the following equation:

$$E = (1 - I_{da}/I_d) \times 100.$$

The correction for light scattering was made by subtracting the signal obtained when unlabeled analogs were incorporated into vesicles containing the donor molecules. A correction for the contribution of the acceptor's emission was made by subtracting the signal produced by the acceptor-labeled analog alone.

RESULTS

The putative membranous segments of ROMK1, namely M1, H5, and M2, were synthesized and fluorescently labeled, and their structure and their abilities to form homo- or heteroaggregates within the membrane were studied. M1 is composed of 26 amino acids, comprising residues 82–107. H5 is a 17-mer polypeptide identical to residues 131–147 of ROMK1, and the third peptide, M2, is composed of 29 amino acids identical to residues 156–184 of ROMK1. These sequences were chosen according to the Kyte and Doolittle hydropathy plot of ROMK1 potassium channel (Kyte and Doolittle, 1982). M1 and M2 were extended at their C-termini with positively charged amino acids (derived from ROMK1 original sequence) to increase their solubilization and thus facilitate their HPLC purification and binding experiments. Fluorescently labeled analogs were prepared by selectively modifying the three peptides at their N-terminal amino acids with either one of the following fluorescent probes: NBD (to serve in the binding experiments and as an energy donor) or Rho (an energy acceptor). The sequences of the peptides, their fluorescently labeled analogs, and their designations are given in Table 1.

CD spectroscopy

The extent of α-helical secondary structure of the peptides was estimated from their CD spectra, as measured in 40% TFE (Fig. 1 *A*) and PC SUV (Fig. 1 B). M1 and M2 exhibited significant CD signals, but H5 did not. Their mean residual ellipticities at Θ_{222} in 40% TFE were −28,650 and −24,000 deg·cm^2/dmol, which correspond to 88% and 73% α-helical content for M1 and M2, respectively. Their mean residual ellipticities at Θ_{222} in PC SUVs were −28,995 and −27,455 deg·cm^2/dmol, which correspond to fractional helicity values of 90% and 85% for M1 and M2, respectively (Wu et al., 1981). Because the CD signal of H5 was very low both in 40% TFE/water and in PC SUVs, it could not be attributed to any particular structure.

TABLE 1 Sequences and designations of the synthetic putative membranous domains of the ROMK1 K^+ channel

No.	Designation	Modification	Sequence
1	M1	X = H	X-HN-^{82}TVFITAFLGSWFLFGL LWYVVAYVHK^{107}-COOH
2	NBD-M1	X = NBD	
3	Rho-H5-M1	X-Rho	
4	H5	X = H	X-HN-^{131}AFLFSLETQVTIGYG FR^{147}-COOH
5	NBD-H5	X = NBD	
6	Rho-H5	X-Rho	
7	M2	X = H	X-HN-^{156}AIFLLIFQSILGVIINSF MCGAILAKISR^{184}-COOH
8	NBD-M2	X = NBD	
9	Rho-M2	X = Rho	
10	Rho-pardaxin	X = Rho	X-HN-GFFALIPKIISSPLFKTL LSAVGSALSSSGGQE-COOH

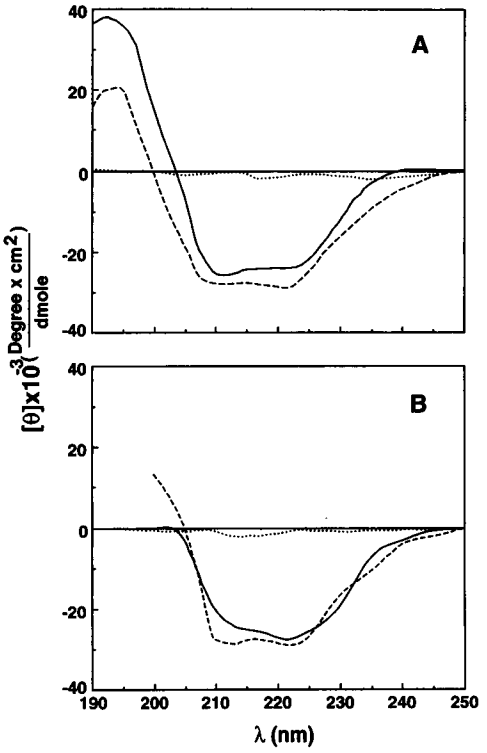

FIGURE 1 CD spectra of ROMK1 peptides. Spectra were taken at peptide concentrations of 0.8–3.0 × 10^{-5} M. – – –, M1; ——, M2; · · · , H5. (*A*) CD of peptides in 40% TFE. (*B*) CD of peptides in 3 mM PC SUV.

Fluorescence measurements of NBD-labeled peptides

The NBD moiety can facilitate determination of the environment of the N-termini of various polypeptides in their membrane-bound state, because its fluorescence intensity is sensitive to the dielectric constant of its surroundings. This probe has already been used in polarity and binding experiments (Kenner and Aboderin, 1971; Frey and Tamm, 1990; Baidin and Huang, 1990; Rapaport and Shai, 1991; Pouny et al., 1992). The fluorescence emission spectra of the three NBD-labeled ROMK1 peptides were measured either in aqueous solutions or in the presence of PC vesicles. All three NBD-labeled segments exhibited fluorescence emission maxima around 550 nm in buffer (Table 2), which agrees with previously reported emission wavelength maxima for NBD derivatives in hydrophilic environments (Rajarathnam et al., 1989; Rapaport and Shai, 1991; Pouny et al., 1992; Gazit and Shai, 1993). However, in solutions of PC vesicles at pH 6.8, the fluorescence emission maxima of NBD-M1, NBD-M2, and NBD-H5 exhibited blue shifts concomitant with increases in their fluorescence intensities (Table 2). The shift was significantly higher for NBD-M1 (λ_{max} = 523 ± 1 nm) than for NBD-M2 (λ_{max} = 533 ± 2) and NBD-H5 (λ_{max} = 533 ± 1 nm). Similar results were

TABLE 2 Emission maxima, the calculated partition coefficients, and free energies of binding of the segments to PC SUVs

Peptide designation	λ_{max} (nm)		K^*_p (M^{-1})	$-\Delta G_{binding}$ (kcal/mol)
	Buffer	PC vesicles	PC vesicles	PC vesicles
NBD-M1	549 ± 1	523 ± 1	0.8 (±0.2) × 10^5 (5)*	9.1
NBD-M2	549 ± 1	533 ± 2	6.0 (±0.5) × 10^5 (4)	10.3
NBD-H5	549 ± 1	533 ± 1	7.3 (±0.8) × 10^5 (5)	10.4
NBD-aminoethanol	546 ± 1	546 ± 1	Not bound	—

*No. of experiments.

observed with PC LUVs (data not shown). Similar magnitudes of blue shifts are observed when surface-active NBD-labeled peptides interact with lipid membranes (Frey and Tamm, 1990; Rapaport and Shai, 1991; Pouny et al., 1992), and are consistent with the NBD probe being located within (in the case of NBD-M1) or on the surface of (in the case of NBD-M2 and NBD-H5) the membrane (Rajarathnam et al., 1989). However, we cannot rule out the possibility that the environment of the NBD moiety is also affected by the intermolecular organization of the membrane-bound peptide. As will be shown in the RET experiments, both M2 and H5 are self-assembled in the membrane, whereas M1 is not. Furthermore, it should be noted that the NBD probe is localized on the N-termini of the peptides, and therefore surface localization of the probe reflects the localization of a particular termini. It does not necessarily reflect the environment of the center of the peptide, which might be dipped within the lipid core of the membrane. In these experiments, the lipid/peptide molar ratio was consistently maintained at an elevated level (3875:1), so that the spectral contribution of free peptide would be negligible.

Tryptophan quenching experiments

A tryptophan residue in the natural sequence of a protein or a peptide can serve as an intrinsic probe for the localization of the peptide within the membrane. M1 contains two tryptophans in the middle of the peptide. When M1 was incorporated into brominated phospholipids, the greatest quenching of tryptophan fluorescence was observed with 11,12 BrPC (1-palmitoyl-2-stearoyl (11–12) dibromo-sn-glycero-3 phosphocoline) and to a lesser degree with 9,10 BrPC (1-palmitoyl-2-stearoyl (9–10) dibromo-sn-glycero-3 phosphocoline) (Fig. 2). No significant quenching of fluorescence was observed with 6,7 BrPC (1-palmitoyl-2-stearoyl (6–7) dibromo-sn-glycero-3 phosphocoline), indicating that the center of the peptide is dipped into the hydrophobic core of the membrane.

Binding experiments

To determine the affinity of the segments for phospholipid membranes, binding experiments were performed as described in the Experimental Procedures. The resulting increases in the fluorescence intensities of the NBD-labeled peptides were plotted as a function of the lipid/peptide molar ratios (see Figs. 3 *A*, 4 *A*, and 5 *A* for NBD-M1, NBD-M2, and NDB-H5, respectively). Binding isotherms were analyzed as partition equilibria as described in the Experimental Procedures. The curves resulting from plotting X^*_b versus free peptide, C_f, are referred to as the conventional binding isotherms and are presented in Figs. 3 *B*, 4 *B*, and 5 *B* for NBD-M1, NBD-M2, and NDB-H5, respectively. The surface partition coefficient of each peptide, K^*_p, was estimated by extrapolating the initial slope of its binding curve to a zero C_f value. The estimated surface partition coefficients (K^*_p) and the calculated free energies of binding ($\Delta G_{binding}$) (Reynolds et al., 1974) of the NBD labeled peptides are listed in Table 2. The values obtained are high and are typical of K^*_p and ($\Delta G_{binding}$) of surface active peptides (Stankowski and Schwarz, 1990; Thiaudiere et al., 1991; Rizzo et al., 1987; Rapaport and Shai, 1991; Pouny and Shai, 1992). It should be noted that the high

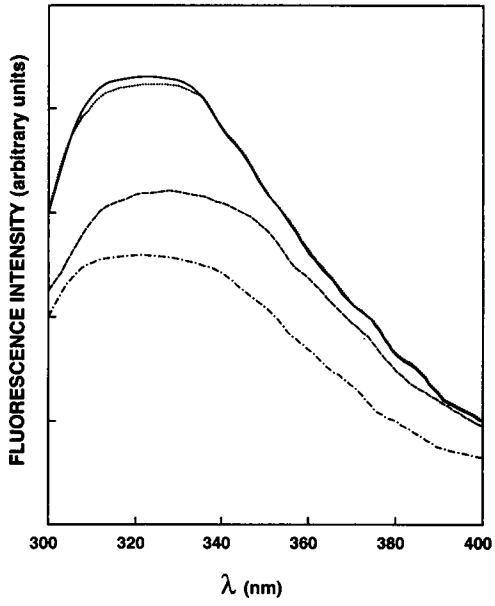

FIGURE 2 Fluorescence emission spectra of 0.25 μM M1. Spectra were determined in the presence of 155 μM PC or BrPC vesicles in buffer composed of 50 mM HEPES-SO_4^{2-}, pH 6.8. The excitation wavelength was set at 280 nm. Emission was scanned from 300–400 nm. M1 in the presence of: PC vesicles (——); 6,7 BrPC (···); 9,10 BrPC (– – –); 11,12 BrPC (– · – · –).

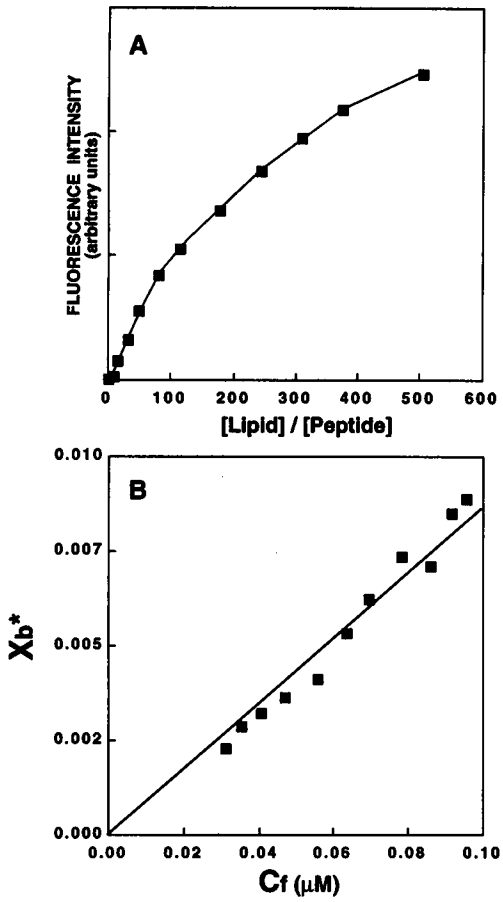

Figure 3

FIGURE 3 Increases in the fluorescence of NBD-M1 upon titration with PC vesicles (*A*), and the resulting binding isotherm (*B*). NBD-M1 (0.1 μM) was titrated with PC SUV with excitation set at 470 nm, and emission was recorded at 530 nm. The experiment was performed at room temperature in 50 mM Na_2SO_4, 25 mM HEPES-SO_4^{-2}, pH 6.8. The binding isotherm was derived from *A* by plotting X_b^* (molar ratio of bound peptide per 60% lipid) versus C_f (equilibrium concentration of free peptide in the solution).

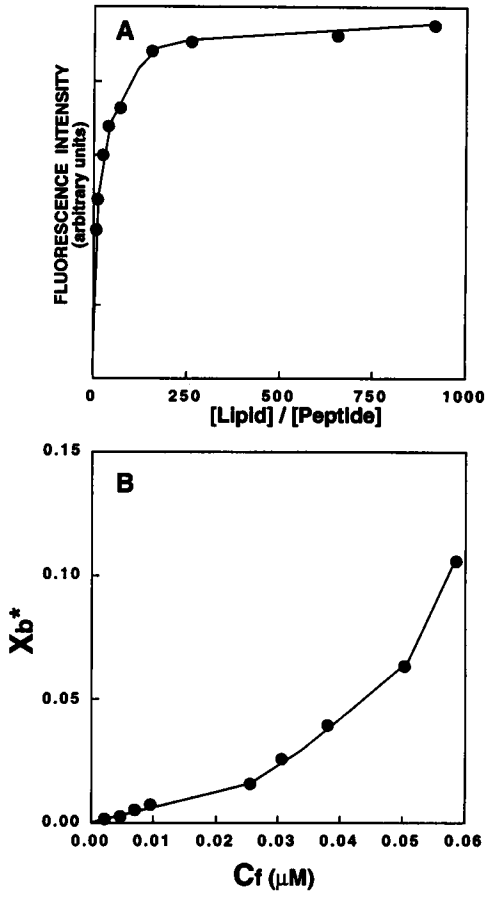

FIGURE 4 Increases in the fluorescence of NBD-M2 upon increasing lipid/peptide molar ratio of PC vesicles (*A*), and the resulting binding isotherm (*B*). As in Fig. 3, except that in this case NBD-M2 (0.04 nmol) was added to increasing concentrations of PC SUV in separate Eppendorf tubes.

quantum yield of the NBD fluorescence in phospholipid membranes facilitates the use of low concentrations of NBD-labeled peptides and thus reduces the aggregation of peptides in solution. However, we cannot rule out the possibility that some aggregation of the peptides occurs in solutions. It should be emphasized also that the purpose of the binding experiments was to determine the lipid/peptide molar ratios at which most of the peptides bind to the membranes. These ratios were then used in the resonance energy transfer experiments to ensure correct calculation of the percentage of energy transfer.

The shape of a binding isotherm of a peptide can provide information on the organization of the peptide within the membrane (Schwarz et al., 1987). The binding isotherms of NBD-M1 and NBD-H5 with the vesicles are straight lines, indicating noncooperativity in the binding process, whereas the binding isotherm of NBD-M2 reflects cooperativity of the binding process (Schwarz et al., 1987).

Energy transfer studies

The curvature of a binding isotherm may indicate whether a particular peptide can form cooperatively large aggregates. To evaluate whether self-association or formation of heteroaggregates between M1, M2, and H5 can occur within membranes at low peptide/lipid molar ratios, RET measurements were performed as described previously (Pouny et al., 1992). For this purpose, the segments were selectively labeled at their N-terminal amino acid, with either NBD (an energy donor) or Rho (an energy acceptor) (Table 1). RET measurements were performed as described in the Experimental Procedures. Examples of typical profiles of the energy transfer from NBD-H5 to Rho-H5, in the presence of PC LUV, are depicted in Fig. 6 *A*; those showing the energy transfer from NBD-H5 to Rho-M2 in the presence of PC phospholipid vesicles are depicted in Fig. 6 *B*; and those showing the energy transfer from NBD-H5 to Rho-M1 are depicted in Fig. 6 *C*. Addition of the various acceptors (final concentration of 0.04 μM or 0.12 μM) to the various donors (final concentration of 0.04 μM) in the presence of PC phospholipid vesicles (156 μM) quenched the donor's emis-

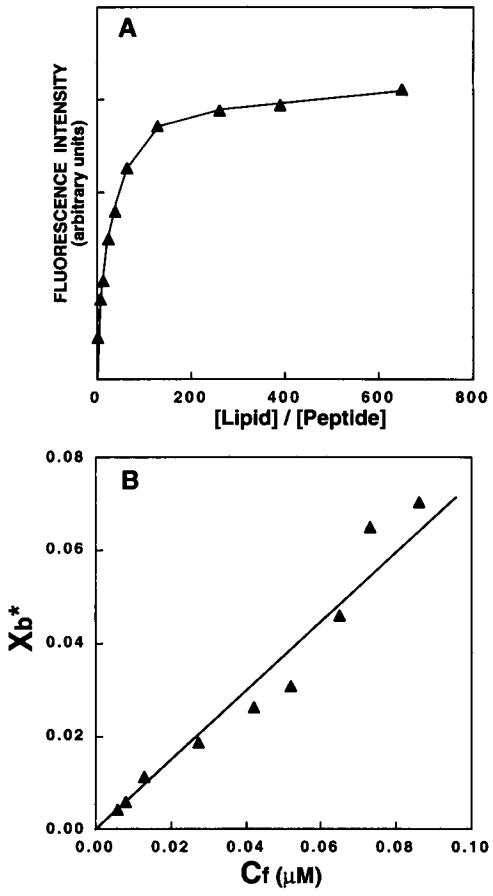

FIGURE 5 Increases in the fluorescence of NBD-H5 upon increasing lipid/peptide molar ratio of PC vesicles (*A*), and the resulting binding isotherm (*B*). See legend to Fig. 3.

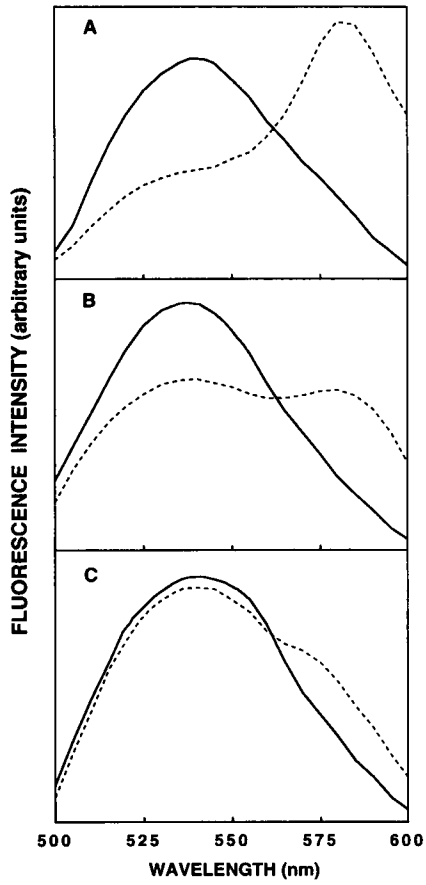

FIGURE 6 Fluorescence energy transfer dependence on Rho-peptide (acceptor) concentrations using PC LUV vesicles. The spectrum of NBD-H5 (0.04 μM), the donor peptide, was determined in the absence (——) or presence (– – –) of 0.012 μM Rho-labeled acceptor peptide. Each spectrum was recorded in the presence of PC vesicles (156 μM) in 50 mM Na_2SO_4, 25 mM HEPES-SO_4^{-2}, at pH 6.8. The excitation wavelength was set at 460 nm. (*A*) In the presence of Rho-H5; (*B*) in the presence of Rho-M2; (*C*) in the presence of Rho-M1. The spectra of Rho-labeled peptides in the presence of vesicles and unlabeled H5 were subtracted from all of the corresponding spectra.

sion and increased the acceptor's emission, which is consistent with energy transfer. The energy transfer was calculated and plotted versus the acceptor/lipid molar ratio (Fig. 7). The lipid/peptide molar ratios in these experiments were kept high (3900:1 and 1300:1) 1) to ensure that practically all of the peptides were in their membrane-bound state and 2) to ensure a low surface density of donors and acceptors, which would reduce energy transfer between unassociated peptide monomers. Adding the acceptor peptide only after the donor peptide was already bound to the membrane prevented any association of the peptides in solution. To confirm that the observed energy transfer was due to aggregation, the transfer efficiencies observed for M1, M2, and H5 were compared with those expected for randomly distributed membrane-bound donors and acceptors (Fig. 7). The random distribution was calculated as described earlier (Fung and Stryer, 1978), and assuming that 51 Å is the R_0 value for the NBD/Rho donor/acceptor pair (Gazit and Shai, 1993). In addition, based on previous calculations made by Tank et al. (1982) and Vaz et al. (1981), the following calculations were made. The diffusion coefficients of phospholipids in fluid bilayers are approximately 1.1×10^{-8} to 3×10^{-8} cm^2/s (Tank et al., 1982; Vaz et al., 1981). For the excited-state lifetime of the donor NBD, $\tau_0 = 7.4 \times 10^{-9}$ s (Chattopadhyay and Mukhrjee, 1993). The mean distance diffused, r, during the lifetime of the donor, which is given in the equation

$$r = [4D\tau_0]^{1/2},$$

is approximately 1.8 Å to 3 Å, which is small compared with the mean distance between the donor and acceptor (225–390 Å). Thus it appears that the monitored RET is due to aggregation and not to random distribution. Fig. 7 illustrates the existence or the lack of energy transfer between the various peptides, namely M1, H5, M2, and pardaxin, which served as an unrelated α-helical peptide inserted into the membrane (Rapaport and Shai, 1991, 1992). The energy transfer observed with the H5/H5, H5/M2, M2/M2, and M1/M2 donor/acceptor pairs was higher than the value expected for a random distribution and was independent of

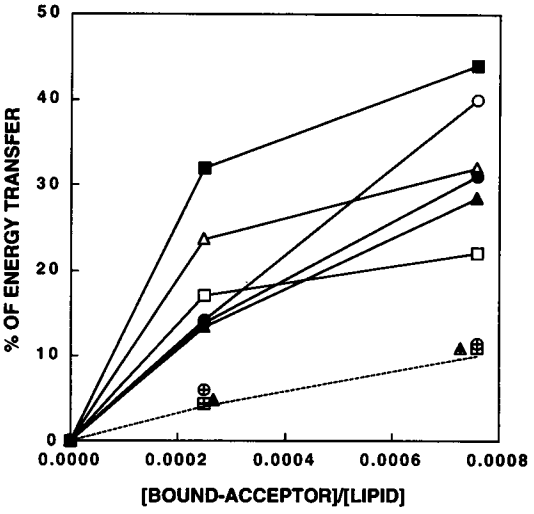

FIGURE 7 Theoretically and experimentally derived percentage of energy transfer. The percentage of energy transfer was calculated as described in the Experimental Procedures and was plotted versus the molar ratio between the bound acceptor and the lipids. The amounts of lipid-bound acceptor (Rho-peptides), C_b, at various acceptor concentrations were calculated from the binding isotherms as described previously (Pouny et al., 1992). ●, NBD-M1/Rho-H5; ▲, NBD-H5/Rho-M2; ■, NBD-H5/Rho-H5; ○, NBD-M2/Rho-H5; □, NBD-M2/Rho-M1; △, NBD-M2/Rho-M2; ⊞, NBD-M2/Rho-pardaxin; ⊕, NBD-H5/Rho-M1; – – –, random distribution of the monomers (Fung and Stryer, 1978), assuming a R_0 of 51 Å. The percentages of RET obtained with NBD-M1/Rho-pardaxin and NBD-H5/Rho-pardaxin pairs fall on the random distribution curve and are not shown to prevent clustering.

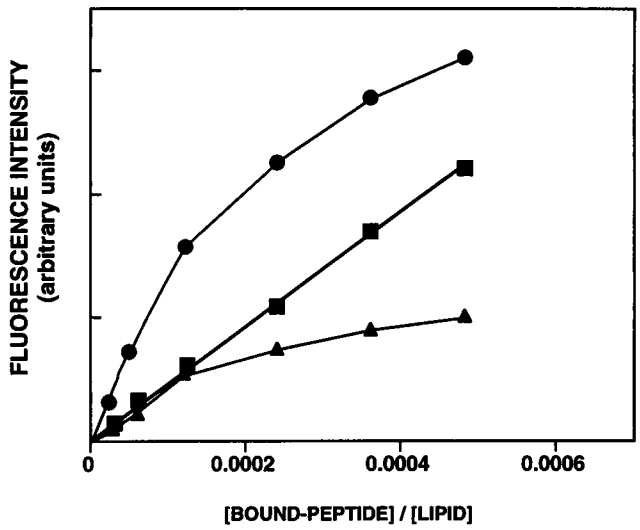

FIGURE 8 Degree of fluorescence intensity as a function of peptide concentration. Fluorescence intensity was plotted versus the molar ratio between the bound NBD-peptide and the lipids. ■, NBD-M1; ▲, NBD-H5; ●, NBD-M2.

whether each of the segments served as a donor or as an acceptor. It should be pointed out that the percentage of RET observed reflects a reduction in the emission fluorescence intesity of the NBD probe as a result of the addition of the acceptor molecules. The random distribution curve was calculated from the decrease in the fluorescence intensity of randomely distributed, and not associated, NBD-labeled molecules due to the addition of nonassociated rhodamine-labled molecules (Fung and Stryer, 1978). However, Fig. 8 reveals that M2 and H5 are already in an aggregation state before the addition of the acceptors (which should also be self-associated at the range of concentrations used in the RET studies). Therefore, the fluorescence of the NBD moeity in the latter case is lower than the value expected if aggregation did not occur. This lower value of the fluorescence causes reduction in the percentage of RET in the case of M2 and H5 as compared to the random distribution curve, and the actual RET should be higher than the experimentally derived values. This suggests that the peptides are associated rather than randomly distributed throughout the membrane. However, with the H5/M1 pair significant energy transfer was observed only when M1 was added first to the vesicle solution either as a donor or as an acceptor. When H5 was added first to the vesicles followed by the addition of M1, the energy transfer resembled that of random distribution (Fig. 7). Random distribution was also observed with the M1/M1 pair. With all the other peptides no change in the emission spectrum was observed when an equal amount of unlabeled acceptor was added instead of the rhodamine-labeled acceptor (data not shown). In control experiments no energy transfer was observed when Rho-pardaxin served as an acceptor to all of the NBD-labeled segments.

The aggregational state of the peptides in the membrane determined by using NBD fluorescence

To further verify the findings in the RET studies that H5 and M2 are self-associated in their membrane-bound state, their NBD-labeled versions were used. The fluorescence intensities of the NBD-labeled peptides were measured as a function of their concentration in PC LUV. The NBD-labeled peptides were incorporated into the vesicles using the same procedure described in the RET experiments. If a particular peptide is not aggregated in membranes, the dose-response curve of its fluorescence intensity should be linear. A deviation from linearity indicates that the peptide is aggregated. The dose-response curves of the fluorescence intensities of the three peptides are shown in Fig. 8. The results reveal that the curves of H5 and M2, but not of M1, deviate from linearity, which agrees with the results obtained in the RET studies, that both H5 and M2 are self-assembled in the membrane, and that M1 is not assembled in the membrane under the same conditions.

DISCUSSION

The assembly of potassium channels is predicted to occur via two steps: first, the folding of the subunit into the correct conformation, followed by the assembly of subunits into

multimeric ion channels (Shen et al., 1993). Increasing evidence is emerging on specific recognition and interaction sites that participate in the oligomerization of ion channels. Such sites have been shown to exist in several cases: in the intracellular domains of potassium ion channels (Li et al., 1992; Shen et al., 1993; Babila et al., 1994), in the acetylcholine receptor α subunit (Yu and Hall, 1994), in the extracellular domains of the acetylcholine receptor subunits (Gu et al., 1991; Yu and Hall, 1991; Sumikawa, 1992; Verrall and Hall, 1992; Chavez et al., 1992), and in the glycine receptor (Kuhse et al., 1993). Subunit interactions sites have also been proposed to exist within the hydrophobic core region of the potassium channel (McCormack et al., 1990; Li et al., 1992). Thus the S1 segment of the potassium channel Kv2.1 has been shown to play a critical role in channel assembly (Babila et al., 1994), as does the M1 segment in the acetylcholine receptor (Yu and Hall, 1994). The transmembrane domains of several other integral membrane proteins have also been implicated in subunit interaction. Examples are glycophorin A (Lemmon et al., 1992; Bormann et al., 1989), bacteriorodopsin (Kahn and Engelman, 1992), the T-cell receptor complex (Bonifacino et al., 1990a,b; Manolios et al., 1990), the lactose permease of *Escherichia coli* (Lynch and Koshland, 1991), the tyrosine kinase receptor family (Sternberg and Gullick, 1990), and the phage M13 coat protein (Deber et al., 1993). Unfortunately, because of the paucity of x-ray diffraction data, high-resolution structures of ion channels as well as of most membrane proteins remain unknown.

In the present study we investigated the structure, in a hydrophobic environment, and the organization within phospholipid membranes of the three putative membranous segments of the ROMK1 channel, namely M1, M2, and H5. Membrane localization of these segments has been predicted previously using hydropathy plots (Ho et al., 1993).

The structure of the segments

Secondary structure determination revealed that both M1 and M2 are predominantly α-helices when in a hydrophobic environment (40% TFE) and phospholipid membranes (Fig. 1). The structure of H5, however, could not be interpreted because the peptide did not yield any significant CD signal. The H5 region of the *Shaker* K^+ channel, which is homologous to H5 of the ROMK1 channel but contains a significant number of amino acids that are not identical, exhibits a low α-helical structure in 1% sodium dodecyl sulfate (Peled and Shai, 1994). Because of the high light scattering in the region of 190–200 nm, this region was omitted from the spectrum. The structural data of M1, M2, and H5 reported herein may aid in the modeling of the structure of the core region of the ROMK1 channel. In support of this, recent studies have shown a correlation between the structure and the organization of synthetic peptides and those of their parent molecules. Such studies were performed for both soluble (Jaenicke, 1991; Kippen et al., 1994; Dyson et al., 1992) and membrane proteins (Kahn and Engelman, 1992; Lemmon and Engelman, 1992; Lomize et al., 1992; Pervushin and Arseniev, 1992; Kaback, 1992; Adair and Engelman, 1994). Other examples come from recent studies showing that various synthetic segments from bacteriorhodopsin (Barsukov et al., 1992), the pore region of δ-endotoxin (Gazit and Shai, 1993), and *Bacillus thuringiensis* var. *israelensis* cytolytic toxin (CytA) (Gazit and Shai, 1993; Li et al., 1996) adopt conformations similar to those of their corresponding segments within the intact protein, as determined by x-ray data.

The organization of the segments within membranes

We demonstrated that synthetic peptides corresponding to putative membranous domains of the ROMK1 channel can self-assemble or coassemble within phospholipid membranes. RET studies reveal that membrane-bound H5 and M2 are self-associated, but that M1 is not (Fig. 7). Moreover, coassembly between H5 and M2 or M1 and M2 appears to be independent of whether the segments serve as donors or acceptors. Interestingly, however, in the case of the H5 and M1 pair, RET is observed only when M1 was added first to the vesicles. A possible interpretation of this finding is as follows. M1, serving as a donor, is randomly distributed in its membrane-bound state (Fig. 7). H5, which is added in the next stage, meets a predominantly monomeric form of M1 and is able to associate with these monomers. This may be a situation in which the channel is still not assembled, and therefore a single subunit that contains only one of each segment is stabilized by the intramembrane domain interactions. However, when H5 serves as a donor and is added first to the vesicle suspension, a large fraction of it is probably self-associated when bound to the membrane (Fig. 7). Indeed, Fig. 8 demonstrates that even at a concentration as low as 0.04 μM (peptide:lipid molar ratio of 0.00024) both H5 and M2 are already aggregated, whereas M1 is not. Therefore, the experimental values of RET obtained when M2 and H5 are used are lower than the real values that would be obtained if the donor peptides were not aggregated at the tested concentration (see details in the Results section). Using lower concentrations of peptides to avoid self-quenching was not possible because the fluorescence intensities were too low. M1, which is added in the next stage, meets a predominantly multimeric form of H5 and is not able to associate with it. This may represent a situation in which the functional channel is formed by the assembly of four subunits (similar to what has been suggested for the *Shaker* K^+ channel; MacKinnon, 1991) and in which the H5 segments of the four subunits are present as a bundle in the lumen of the channel. In that case only M2 could recognize this bundle of H5. The relatively hydrophilic environment of the N-terminus of M2 (λ_{max} = 533 ± 2, Table 2) may indicate that when the bundle of the M2 segments is formed, the

N-termini of the segments are either exposed to the surface of the membrane or buried in the hydrophilic environment formed in the interior of the bundle.

The self-association of the H5 and M2 segments and the ability of the segments to form heteroaggregates in their membrane-bound state appear to be at least partially specific, because neither one of the segments associates with membrane-bound pardaxin (which also adopts an α-helical structure and is membrane embedded; Rapaport and Shai, 1991) (Fig. 7). These findings suggest that M2 and H5 form the inner part of the pore and that M1 participates in the formation of the outer ring of α-helices. In support of this, recent findings demonstrated that a single mutation within the M2 transmembrane segment of ROMK1 and IRK1 affects the strength of rectification (Lu and MacKinnon, 1994; Wible et al., 1994) and the voltage gating (Wible et al., 1994) of these channels, therefore suggesting that the side chain of the mutated amino acid within M2 is in contact with the aqueous pore (Lu and MacKinnon, 1994). Because M2 is uncharged, its self-assembly is probably mediated mostly through the hydrophobic residues, as in the phage M13 coat protein (Deber et al., 1993) and in contrast, for example, to charge attraction in the transmembrane domain of the T-cell receptor complex (Bonifacino et al., 1990a,b; Manolios et al., 1990). Charge interactions were also recently found between the S4 and S3 of the *Shaker* K^+ channel, both in the intact channel (Papazian et al., 1995; Planells-Cases et al., 1995) and between the synthetic peptides (Peled-Zehavi et al., 1996).

There is strong evidence that the interactions between the peptides studied herein occur within the membrane milieu. NBD shift experiments (Table 2) as well as tryptophan quenching experiments (Fig. 3) indicated that M1 is inserted into the membrane. Enzymatic cleavage experiments of these peptides (data not shown) indicated that they are not cleaved from the membrane by proteinase K, in spite of the relatively small NBD shift of M2 and H5. In addition, the interaction of M2 with M1 in their membrane-bound state did not affect the fluorescence of the NBD probe attached to the inserted M1, suggesting that the interaction is within the hydrophobic core of the membrane. The equilibrium constants for the aggregation between the different pairs of peptides cannot be derived based on the RET studies, because their calculation requires knowledge of the amount of assembled heteroaggregates, their exact stoichiometry, as well as the aggregational state of each one of the peptides, parameters that are not known and cannot be simply derived from the RET results. This is partially because, as discussed in the section of the RET studies, the experimental percentages of energy transfer observed (Fig. 7) were lower than the values that should be obtained if the donors and the acceptors were not aggregated in the membrane. Therefore, even in the case of a homogeneous system containing only H5 or M2, these values cannot be used to estimate the amount of associated peptides. However, recent studies on the reversible aggregation in pore formation by the cytolytic peptide pardaxin, based on the estimation of the size of the aggregates required to cause ion leakage from vesicles, yielded an association constant for pardaxin molecules on the order of 10^3 to 10^4 M^{-1} (Rapaport et al., 1996). Because pardaxin assembles in membrane at concentrations similar to those reported herein for the ROMK1 segments, it is reasonable to assume that the association constants for these peptides are also on the same order of magnitude.

Very recently Taglialatela and colleagues found that the carboxy terminus of IRK1 appears to have a major role in specifying some of the pore properties of IRK1, such as inward rectification and single-channel conductance, but not selectivity (Taglialatela et al., 1994). Thus it is possible that the pore may also be made up of other segments of the protein. Experiments are being conducted to evaluate the existence, in the C-termini of IRK1 and ROMK1, of other segments that interact with the membrane and with the pore-forming region.

This research was supported in part by grants from the Pearl Levine Foundation for Research in the Neurosciences, the Basic Research Foundation administered by the Israel Academy of Sciences and Humanities, and the MINERVA Foundation, Munich, Germany.

REFERENCES

Adair, B. D., and D. M. Engelman. 1994. Glycophorin A helical transmembrane domains dimerize in phospholipid bilayers: a resonance energy transfer study. *Biochemistry.* 33:5539–5544.

Ashford, M. L., C. T. Bond, T. A. Blair, and J. P. Adelman. 1994. Cloning and functional expression of a rat heart KATP channel. *Nature.* 370: 456–459.

Babila, T., A. Moscucci, H. Wang, F. E. Weaver, and G. Koren. 1994. Assembly of mammalian voltage-gated potassium channels: evidence for an important role of the first transmembrane segment. *Neuron.* 12:615–626.

Baidin, G., and J. R. Huang. 1990. Fluorescence properties of the Ca^{2+},Mg^{2+}-ATPase protein of sarcoplasmic reticulum labeled with 7-chloro-4-nitrobenzo-2-oxa-1,3-diazole. *FEBS Lett.* 259:254–256.

Barsukov, I. L., D. E. Nolde, A. L. Lomize, and A. S. Arseniev. 1992. Three-dimensional structure of proteolytic fragment 163–231 of bacteriorodopsin determined from nuclear magnetic resonance data in solution. *Eur. J. Biochem.* 206:665–672.

Bartlett, G. R. 1959. Phosphoros assay in column chromatography. *J. Biol. Chem.* 234:466–468.

Ben-Efraim, I., D. Bach, and Y. Shai. 1993. Spectroscopic and functional characterization of the putative transmembrane segment of the minK potassium channel. *Biochemistry.* 32:2371–2377.

Beschiaschvili, G., and J. Seelig. 1990. Melittin binding to mixed phosphatidylglycerol/phosphatidylcholine membranes. *Biochemistry.* 29:52–58.

Bolen, E. J., and P. W. Holloway. 1990. Quenching of tryptophan fluorescence by brominated phospholipid. *Biochemistry.* 29:9638–9643.

Bonifacino, J. S., P. Cosson, and R. D. Klausner. 1990a. Colocalized transmembrane determinants for ER degradation and subunit assembly explain the intracellular fate of TCR chains. *Cell.* 63:503–513.

Bonifacino, J. S., C. K. Suzuki, and R. D. Klausner. 1990b. A peptide sequence confers retention and rapid degredation in the endoplasmic reticulum. *Science.* 247:79–82.

Bormann, B. J., W. J. Knowles, and V. T. Marchesi. 1989. Synthetic peptides mimic the assembly of transmembrane glycoproteins. *J. Biol. Chem.* 264:4033–4037.

Butler, A., A. G. Wei, K. Baker, and L. Salkoff. 1989. A family of putative potassium channel genes in Drosophila. *Science.* 243:943–947.

Chattopadhyay, A., and S. Mukhrjee. 1993. Fluorophore environments in membrane-bound probes: a red edge excitation shift study. *Biochemistry.* 32:3804–3811.

Chavez, R. A., J. Maloof, D. Beeson, D. J. Newsom, and Z. W. Hall. 1992. Subunit folding and alpha delta heterodimer formation in the assembly of the nicotinic acetylcholine receptor. Comparison of the mouse and human alpha subunits. *J. Biol. Chem.* 267:23028–23034.

Chen, Y. H., J. T. Yang, and K. H. Chau. 1974. Determination of the helix and beta form of proteins in aqueous solution by circular dichroism. *Biochemistry.* 13:3350–3359.

Dascal, N., N. F. Lim, W. Schreibmayer, W. Wang, N. Davidson, and H. A. Lester. 1993. Expression of an atrial G-protein-activated potassium channel in Xenopus oocytes. *Proc. Natl. Acad. Sci. USA.* 90: 6596–6600.

Deber, C. M., A. R. Khan, Z. Li, C. Joensson, M. Glibowicka, and J. Wang. 1993. Val→Ala mutations selectively alter helix-helix packing in the transmembrane segment of phage M13 coat protein. *Proc. Natl. Acad. Sci. USA.* 90:11648–11652.

De Kroon, A. I., M. W. Soekarjo, J. De Gier, and B. De Kruijff. 1990. The role of charge and hydrophobicity in peptide-lipid interaction: a comparative study based on tryptophan fluorescence measurements combined with the use of aqueous and hydrophobic quenchers. *Biochemistry.* 29:8229–8240.

Dyson, H. J., J. R. Sayre, G. Merutka, H. C. Shin, R. A. Lerner, and P. E. Wright. 1992. Folding of peptide fragments comprising the complete sequence of proteins. Models for initiation of protein folding. II. Plastocyanin. *J. Mol. Biol.* 226:819–835.

Frey, S., and L. K. Tamm. 1990. Membrane insertion and lateral diffusion of fluorescence-labelled cytochrome c oxidase subunit IV signal peptide in charged and uncharged phospholipid bilayers. *Biochem. J.* 272: 713–719.

Fung, B. K., and L. Stryer. 1978. Surface density determination in membranes by fluorescence energy. *Biochemistry.* 17:5241–5248.

Gazit, E., and Y. Shai. 1993. Structural and functional characterization of the alpha 5 segment of *Bacillus thuringiensis* delta-endotoxin. *Biochemistry.* 32:3429–3436.

Gazit, E., and Y. Shai. 1993. Structural characterization, membrane interaction, and specific assembly within phospholipid membranes of hydrophobic segments from *Bacillus thuringiensis* var. *israelensis* cytolytic toxin. *Biochemistry.* 32:12363–12371.

Gonzalez-Manas, J. M., J. H. Lakey, and F. Pattus. 1992. Brominated phospholipids as a tool for monitoring the membrane insertion of colicin A. *Biochemistry.* 31:7294–7300.

Greenfield, N., and G. D. Fasman. 1969. Computed circular dichroism spectra for the evaluation of protein conformation. *Biochemistry.* 8:4108–4116.

Gu, Y., J. R. Forsayeth, S. Verrall, X. M. Yu, and Z. W. Hall. 1991. Assembly of the mammalian muscle acetylcholine receptor in transfected COS cells. *J. Cell. Biol.* 114:799–807.

Harris, R. W., P. J. Sims, and R. K. Tweten. 1991. Kinetic aspects of the aggregation of clostridium perfringens theta-toxin in erythrocyte membrane. A fluorescence energy transfer study. *J. Biol. Chem.* 266: 6936–6941.

Hille, B. 1992. Ionic Channels of Excitable Membranes, 2nd Ed. Sinauer Associates, Sunderland, MA.

Ho, K., C. G. Nichols, W. J. Lederer, J. Lytton, P. M. Vassilev, M. V. Kanazirska, and S. C. Hebert. 1993. Cloning and expression of an inwardly rectifying ATP-regulated potassium channel. *Nature.* 362: 31–38.

Hope, M. J., M. B. Bally, G. Webb, and P. R. Cullis. 1985. Production of large unilamellar vesicles by a rapid extrusion procedure. Characterization of size distribution, trapped volume and ability to maintain a membrane potential. *Biochim. Biophys. Acta.* 812:55–65.

Jaenicke, R. 1991. Protein folding: local structures, domains, subunits, and assemblies. *Biochemistry.* 30:3147–3161.

Kaback, H. R. 1992. The lactose permease of *Escherichia coli*: a paradigm for membrane transport proteins. *Biochim. Biophys. Acta.* 1101: 210–213.

Kahn, T. W., and D. M. Engelman. 1992. Bacteriorhodopsin can be refolded from two independently stable transmembrane helices and the complementary five-helix fragment. *Biochemistry.* 31:6144–6151.

Kenner, R. A., and A. A. Aboderin. 1971. A new fluorescent probe for protein and nucleoprotein conformation. Binding of 7-(*p*-methoxybenzylamino)-4-nitrobenzoxadiazole to bovine trypsinogen and bacterial ribosomes. *Biochemistry.* 10:4433–4440.

Kippen, A. D., V. L. Arcus, and A. R. Fersht. 1994. Structural studies on peptides corresponding to mutants of the major α-helix of barnase. *Biochemistry.* 33:10013–10021.

Kubo, Y., T. J. Baldwin, Y. N. Jan, and L. Y. Jan. 1993a. Primary structure and functional expression of a mouse inward rectifier potassium channel. *Nature.* 362:127–133.

Kubo, Y., E. Reuveny, P. A. Slesinger, Y. N. Jan, and L. Y. Jan. 1993b. Primary structure and functional expression of a rat G-protein-coupled muscarinic potassium channel [see comments]. *Nature.* 364:802–806.

Kuhse, J., B. Laube, D. Magalei, and H. Betz. 1993. Assembly of the inhibitory glycine receptor: identification of amino acid sequence motifs governing subunit stoichiometry. *Neuron.* 11:1049–1056.

Kyte, J., and R. F. Doolittle. 1982. A simple method for displaying the hydropathic character of a protein. *J. Mol. Biol.* 157:105–132.

Lelkes, P. I. 1984. Liposome Technology. CRC Press, Boca Raton, FL.

Lemmon, M. A., and D. M. Engelman. 1992. Helix-helix interactions inside lipid bilayers. *Curr. Opin. Struct. Biol.* 2:511–518.

Lemmon, M. A., J. M. Flanagan, J. F. Hunt, B. D. Adair, B. J. Bormann, C. E. Dempsey, and D. M. Engelman. 1992. Glycophorin A dimerization is driven by specific interactions between transmembrane α-helices. *J. Biol. Chem.* 267:7683–7689.

Li, M., Y. N. Jan, and L. Y. Jan. 1992. Specification of subunit assembly by the hydrophilic amino-terminal domain of the Shaker potassium channel. *Science.* 257:1225–1230.

Li, J. D., P. A. Koni, and D. J. Ellar. 1996. Structure of the Mosquitocidal delta-endotoxin CytB from *Bacillus thuringiensis* ssp. *kyushuensis* and implications for membrane pore formation. *J. Mol. Biol.* 257:129–152.

Lomize, A. L., K. V. Pervushin, and A. S. Arseniev. 1992. Spatial structure of (34–65)bacterioopsin polypeptide in SDS micelles determined from nuclear magnetic resonance data. *J. Biomol. NMR.* 2:361–372.

Lu, Z., and R. MacKinnon. 1994. Electrostatic tuning of Mg^{2+} affinity in an inward-rectifier K^+ channel. *Nature.* 371:243–246.

Lynch, B. A., and D. E. Koshland, Jr. 1991. Disulfide cross-linking studies of the transmembrane regions of the aspartate sensory receptor of *Escherichia coli. Proc. Natl. Acad. Sci. USA.* 88:10402–10406.

MacKinnon, R. 1991. Determination of the subunit stoichiometry of a voltage-activated potassium channel. *Nature.* 350:232–235.

Manolios, N., J. S. Bonifacino, and R. D. Klausner. 1990. Transmembrane helical interactions and the assembly of the T cell receptor complex. *Science.* 249:274–277.

McCormack, K., J. W. Lin, L. E. Iverson, and B. Rudy. 1990. *Shaker* potassium channel subunits form heteromultimeric channels with novel functional properties. *Biochem. Biophys. Res. Commun.* 171:1361–1371.

Merrifield, R. B., L. D. Vizioli, and H. G. Boman. 1982. Synthesis of the antibacterial peptide cecropin A (1–33). *Biochemistry.* 21:5020–5031.

Miller, C. 1991. 1990: annus mirabilis of potassium channels. *Science.* 252:1092–1096.

Papahadjopoulos, D., and N. Miller. 1967. Phospholipid model membranes. I. Structural characteristics of hydrated liquid crystals. *Biochim. Biophys. Acta.* 135:624–638.

Papazian, D. M., X. M. Shao, S. A. Seo, A. F. Mock, Y. Huang, and D. H. Wainstock. 1995. Electrostatic interactions of S4 voltage sensor in *Shaker* K^+ channel. *Neuron.* 14:1293–1301.

Peled, H., and Y. Shai. 1994. Synthetic S-2 and H-5 segments of the Shaker K^+ channel: secondary structure, membrane interaction, and assembly within phospholipid membranes. *Biochemistry.* 33:7211–7219.

Peled-Zehavi, H., I. T. Arkin, D. M. Engelman, and Y. Shai. 1996. Coassembly of synthetic segments of *Shaker* K^+ channel within phospholipid membranes. *Biochemistry.* 35:6828–6838.

Pervushin, K. V., and A. S. Arseniev. 1992. Three-dimensional structure of (1–36)bacterioopsin in methanol-chloroform mixture and SDS micelles determined by 2D ^{1}H-NMR spectroscopy. *FEBS Lett.* 308:190–196.

Planells-Cases, R., A. V. Ferrer-Montiel, C. D. Patten, and M. Montal. 1995. Mutation of conserved negatively charged residues in the S2 and S3 transmembrane segments of a mammalian K^+ channel selectively modulates channel gating. *Proc. Natl. Acad. Sci. USA.* 92:9422–9426.

Pouny, Y., D. Rapaport, A. Mor, P. Nicolas, and Y. Shai. 1992. Interaction of antimicrobial dermaseptin and its fluorescently labeled analogues with phospholipid membranes. *Biochemistry.* 31:12416–12423.

Pouny, Y., and Y. Shai. 1992. Interaction of D-amino acid incorporated analogues of pardaxin with membranes. *Biochemistry.* 31:9482–9490.

Rajarathnam, K., J. Hochman, M. Schindler, and S. Ferguson-Miller. 1989. Synthesis, location, and lateral mobility of fluorescently labeled ubiquinone 10 in mitochondrial and artificial membranes. *Biochemistry.* 28: 3168–3176.

Rapaport, D., R. Peled, S. Nir, and Y. Shai. 1996. Reversible surface aggregation in pore formation by pardaxin. *Biophys. J.* 70:1–11.

Rapaport, D., and Y. Shai. 1991. Interaction of fluorescently labeled pardaxin and its analogues with lipid bilayers. *J. Biol. Chem.* 266: 23769–23775.

Rapaport, D., and Y. Shai. 1992. Aggregation and organization of pardaxin in phospholipid membranes. A fluorescence energy transfer study. *J. Biol. Chem.* 267:6502–6509.

Reynolds, J. A., D. B. Gilbert, and C. Tanford. 1974. Empirical correlation between hydrophobic free energy and aqueous cavity. *Proc. Natl. Acad. Sci. USA.* 71:2925–2927.

Rizzo, V., S. Stankowski, and G. Schwarz. 1987. Alamethicin incorporation in lipid bilayers: a thermodynamic study. *Biochemistry.* 26: 2751–2759.

Schwarz, G., H. Gerke, V. Rizzo, and S. Stankowski. 1987. Incorporation kinetics in a membrane, studied with the pore-forming peptide alamethicin. *Biophys. J.* 52:685–692.

Schwarz, G., S. Stankowski, and V. Rizzo. 1986. Thermodynamic analysis of incorporation and aggregation in a membrane: application to the pore-forming peptide alamethicin. *Biochim. Biophys. Acta.* 861: 141–151.

Schwarz, T. L., B. L. Tempel, D. M. Papazian, Y. N. Jan, and L. Y. Jan. 1988. Multiple potassium-channel components are produced by alternative splicing at the Shaker locus in Drosophila. *Nature.* 331:137–142.

Shai, Y., Y. R. Hadari, and A. Finkels. 1991. pH-dependent pore formation properties of pardaxin analogues. *J. Biol. Chem.* 266:22346–22354.

Shen, N. V., X. Chen, M. M. Boyer, and P. J. Pfaffinger. 1993. Deletion analysis of K^+ channel assembly. *Neuron.* 11:67–76.

Sheng, M., Y. J. Liao, Y. N. Jan, and L. Y. Jan. 1993. Presynaptic A-current based on heteromultimeric K^+ channels detected in vivo. *Nature.* 365:72–75.

Stankowski, S., and G. Schwarz. 1990. Electrostatics of a peptide at a membrane/water interface. The pH dependence of melittin association with lipid vesicles. *Biochim. Biophys. Acta.* 1025:164–172.

Sternberg, M. J. E., and W. J. Gullick. 1990. A sequence motif in the transmembrane region of growth factor receptors with tyrosine kinase activity mediates dimerization. *Protein Eng.* 3:245–248.

Stühmer, W., F. Conti, H. Suzuki, X. Wang, M. Noda, N. Yahadi, H. Kubo, and S. Numa. 1989. Structural parts involved in activation and inactivation of the sodium channel. *Nature.* 339:597–603.

Sumikawa, K. 1992. Sequences on the N-terminus of ACh receptor subunits regulate their assembly. *Brain Res. Mol. Brain Res.* 13:349–353.

Suzuki, M., K. Takahashi, M. Ikeda, H. Hayakawa, A. Ogawa, Y. Kawaguchi, and O. Sakai. 1994. Cloning of a pH-sensitive K^+ channel possessing two transmembrane segments. *Nature.* 367:642–645.

Taglialatela, M., B. A. Wible, R. Caporaso, and A. M. Brown. 1994. Specification of pore properties by the carboxyl terminus of inwardly rectifying K^+ channels. *Science.* 264:844–847.

Tank, D. W., E. S. Wu, P. R. Meers, and W. W. Webb. 1982. Lateral diffusion of gramicidine C in phospholipid multibilayers. Effects of cholesterol and high gramicidin concentration. *Biophys. J.* 40:129–135.

Thiaudiere, E., O. Siffert, J. C. Talbot, J. Bolard, J. E. Alouf, and J. Dufourcq. 1991. The amphiphilic alpha-helix concept. Consequences on the structure of staphylococcal delta-toxin in solution and bound to lipids. *Eur. J. Biochem.* 195:203–213.

Tytgat, J., J. Vereecke, and E. Carmeliet. 1994. Reversal of rectification and alteration of selectivity and pharmacology in a mammalian Kv1.1 potassium channel by deletion of domains S1 to S4. *J. Physiol. (Lond.).* 481:7–13.

Vaz, W. L. C., H. G. Kapitza, J. E. Steumpel Sackmann, and T. M. Jovin. 1981. Translatonal mobolity of glycerophorin in bilayer membranes of dimyristoylphosphatidylcholine. *Biochemistry.* 20:1392–1396.

Verrall, S., and Z. W. Hall. 1992. The N-terminal domains of acetylcholine receptor subunits contain recognition signals for the initial steps of receptor assembly. *Cell.* 68:23–31.

Wang, H., D. D. Kunkel, T. M. Martin, P. A. Schwartzkroin, and B. L. Tempel. 1993. Heteromultimeric K^+ channels in terminal and juxtaparanodal regions of neurons. *Nature.* 365:75–79.

Wible, B. A., M. Taglialatela, E. Ficker, and A. M. Brown. 1994. Gating of inwardly rectifying K^+ channels localized to a single negatively charged residue. *Nature.* 371:246–249.

Wu, C. S. C., K. Ikeda, and J. T. Yang. 1981. Ordered conformation of polypeptides and proteins in acidic dodecyl sulfate solution. *Biochemistry.* 20:566–570.

Yu, X. M., and Z. W. Hall. 1991. Extracellular domains mediating epsilon subunit interactions of muscle acetylcholine receptor. *Nature.* 352: 64–67.

Yu, X. M., and Z. W. Hall. 1994. A sequence in the main cytoplasmic loop of the alpha subunit is required for assembly of mouse muscle nicotinic acetylcholine receptor. *Neuron.* 13:247–255.